ZESZYTY NAUKOWE POLITECHNIKI ŚLĄSKIEJ 2003
Seria: GÓRNICTWO z. 257 Nr kol. 1599

Stanisław F. ŚCIESZKA
Politechnika Śląska

TESTING MECHANICAL PROPERTIES OF MATERIALS FOR MINING TOOLS. FRACTURE TOUGHNESS MEASUREMENT METHODS – A REVIEW

Summary. Techniques for fracture toughness evaluation of materials for mining and drilling tools are extensively discussed in this paper. To aid work, a simple and reliable testing methods for fracture toughness, and abrasive wear or alternatively the integrated testing method, in which a conjoint action involving both fracture and abrasion occur are needed.

BADANIA WŁASNOŚCI MECHANICZNYCH MATERIAŁÓW NA NARZĘDZIA GÓRNICZE. PRZEGLĄD METOD WYZNACZANIA ODPORNOŚCI NA KRUCHE PĘKANIE

Streszczenie. Praca zawiera obszerny przegląd metod stosowanych do badania odporności na kruche pękanie materiałów na ostrza narzędzi górniczych i wiertniczych. Rozwój węglików spiekanych stworzył potrzebę opracowania nowej i szybkiej metody badania najważniejszych własności powyższych materiałów, czyli ich odporności na kruche pękanie i odporności na zużywanie ścierne oraz docelowo zaproponowanie metody integrującej oba mechanizmy niszczenia.

1. Introduction

The properties of tungsten carbide cobalt (WC-Co) have been extensively studied [1-5], due to its importance in industrial applications. Hardmetals have a variety of applications, and the requirements of their properties may vary with application. The mechanical properties, such as wear resistance and fracture toughness are in many cases directly related to their performance in industrial application. Hence fracture toughness and wear resistance are two

of the major materials characteristics to take into consideration when designing e.g. mining tools, particularly inserts for rotary and percussion-rotary drilling, inserts for mining shearer picks and rotary picks [6, 7] made of hardmetals. This is mainly due to the risk of brittle fracture in tools made of these materials and due to the importance of resistance to abrasion action where the content pressure between the component and abrasive is high, such as in mining and rock drilling.

WC-Co hardmetals are materials that combine high abrasion resistance and hardness with rather low levels of toughness which tend to decrease as hardness increase. Nevertheless, the main problem facing designers remains the fact that the tungsten carbide tools may exhibit sudden brittle fracture at high stresses such as are encountered in rock drilling and cutting. In rock drilling the motion of the bit is seemingly uniform and contact between the bit and rock steadily builds up force until the compressive or shear yield strength of the rock is reached and rock is moved out of the way of the bit. Although the operating conditions vary from one design to another, all drag bits produce holes by one or more of three mechanisms: dislodging of granular rock, shearing of brittle rock, and ploughing. During these interactions, the large forces which can build up can cause the above mentioned fracture or extreme bit wear [6].

As stated above, rock drilling and cutting produce both impact and abrasion in various relative amounts at the tool/rock interface mainly because of the rock fragmentation itself is a discrete process rather than a continuous one. Depending on operating conditions and different rock materials, the following wear modes can be observed [7, 8]:

1. microfracturing and chipping of the tungsten carbide grains,
2. plastic grooving and polishing of carbide grains, with compacting of powder rock debris over the face of the carbide [9], together with metallic binder phase extraction and preferential removal and intergranular spalling of the surface;
3. transgranular fracture of tungsten carbide grains,
4. thermal fatigue leading to intergranular cracking.

Since the fracture toughness is often the major limiting parameter governing the use of WC-Co drilling, cutting and other tools, there is a need for research aimed at increasing toughness without sacrificing wear resistance. To aid in this objective, a simple and reliable integrated testing method, in which a conjoint action involving both fracture and abrasion occur, is needed for quick assessment of progress in such research. Techniques for fracture toughness evaluation and abrasive wear measurement are discussed in this paper and the new integrated testing method currently developed [10, 11] is proposed for further, more advanced study in the paper [27]. The method is based on the concept of edge chipping during the initial

transition stage of abrasion wear which is controlled by brittle fracture process. Although the method of testing is not yet well established it is seen as a promising and pragmatic way of ranking hard materials for fracture toughness and wear resistance. The limitations of the method for tougher materials [12] such as tool steels as well as for very brittle materials such as ceramics were not yet investigated and determined.

2. Fracture toughness measurement methods

For metallic materials, fracture toughness is conventionally determined by methods well documented in ASTM E399 and ASTM E1820 and their derivatives. These standardised plane strain fracture tests produce K_{IC} value. Toughness is therefore essentially defined as the resistance to propagation of a pre-existing crack of known dimensions, and is usually expressed in terms of a critical crack tip stress intensity factor, K_{IC}:

$$K_{IC} = Y C^{\frac{1}{2}} \sigma_C \qquad (1)$$

where Y is a crack geometry parameter, C is the crack length, and σ_C is the applied stress normal to the crack plane at fracture for the so-called opening mode (mode I). But there are also alternative expressions for toughness such as strain energy release rate, $G = K_C^2 / E(1-\nu^2)$, where ν is the Poisson's ratio and E is Young's modulus.

Many of these methods need adaptation for use with hard materials (hardmetals, advanced technical ceramics and cermets) because testpieces tend to be impractically large or pre-cracking is more difficult, than for metallic materials.

Over the last decade there have been useful developments in methods of testing specifically for advanced technical ceramics and hardmetals. There is a considerable body of published information on these methods, e.g. comprehensive reviews are included in NPL Measurement Good Practice Guides [1, 2, 4, 13]. This wide variety of methods is suitable rather exclusively for low toughness material. Figure 1 shows them schematically. Many of them are based on flexural strength testpieces, especially if the material has a moderate grain size or texture. The methods are as follows:

SEPB Single Edge Pre-cracked Beam (Fig. 1a). Beam with sharp crack on tensile surface. Hardmetals are difficult to pre-crack. Pre-cracking requires some skill to obtain straight-fronted cracks. Results are influenced by rising crack resistance behaviour. Standards (ASTM C1421, JIS R1607, ISO 15732).

CNB Chevron Notched Beam (Fig. 1b). Flexural beam with two coplanar angled notches leaving a sharp-tipped triangular shaped region to fracture. Crack initiation difficult in hardmetals, not recommended. Results are influenced by rising crack resistance behaviour. Standards (ASTM C1421).

SCF Surface Crack-in Flexure (Fig. 1c). Flexural beam test in which a small semicircular flaw has been introduced by indentation on the tensile side. It is not possible to remove surface damage in hardmetals and leave a useful pre-crack. Not recommended for hardmetals. Standards (ASTM 1421).

SEVNB Single Edge V-notched Beam (Fig. 1d). Flexural beam test in which a narrow notch made on the tensile side has its tip sharpened by honing with diamond paste. Validated on ceramics. More work needed on hardmetals to confirm requisite notch sharpness. Standards (provisional standard number not yet allocated).

IF Indentation Fracture (Fig. 1e). Palmqvist toughness test. A test in which the length of cracks emanating from the corners of a Vickers hardness indentation is measured. Works reasonably well for hardmetals in toughness range 10-16 $MNm^{-3/2}$ provided that the surface is free from residual stresses. Generally it is recommended that this method is not used for definitive data, but is used only for comparative purposes. Tougher materials produce few or inconsistently sized cracks. Standards (JIS R1607).

IS Indentation Strength (Fig. 1f). A flexural test on a beam into which has been placed an indentation on the tensile side. Damage and residual stresses associated with indentation have strong influence on results. Not recommended for hardmetals and again, this method should not be used for obtaining definitive data, but is used only as a comparative method. Standards (provisional standards number not yet allocated).

DCB Double Cantilever Beam (Fig. 1g). This plate method has several variants, and has not been standardised except for metallic testpiece (ASTM E399). Testpieces need to be carefully machine, and an appropriate means of pulling them introduced. The method is not widely used because of the large quantity of material that is required for a single determination.

DT Double Torsion (Fig. 1h). This plate method is simple to undertake than the double cantilever beam method. Useful for slow crack growth behaviour. Crack front not straight, and obtaining the effective length may require a compliance calibration.

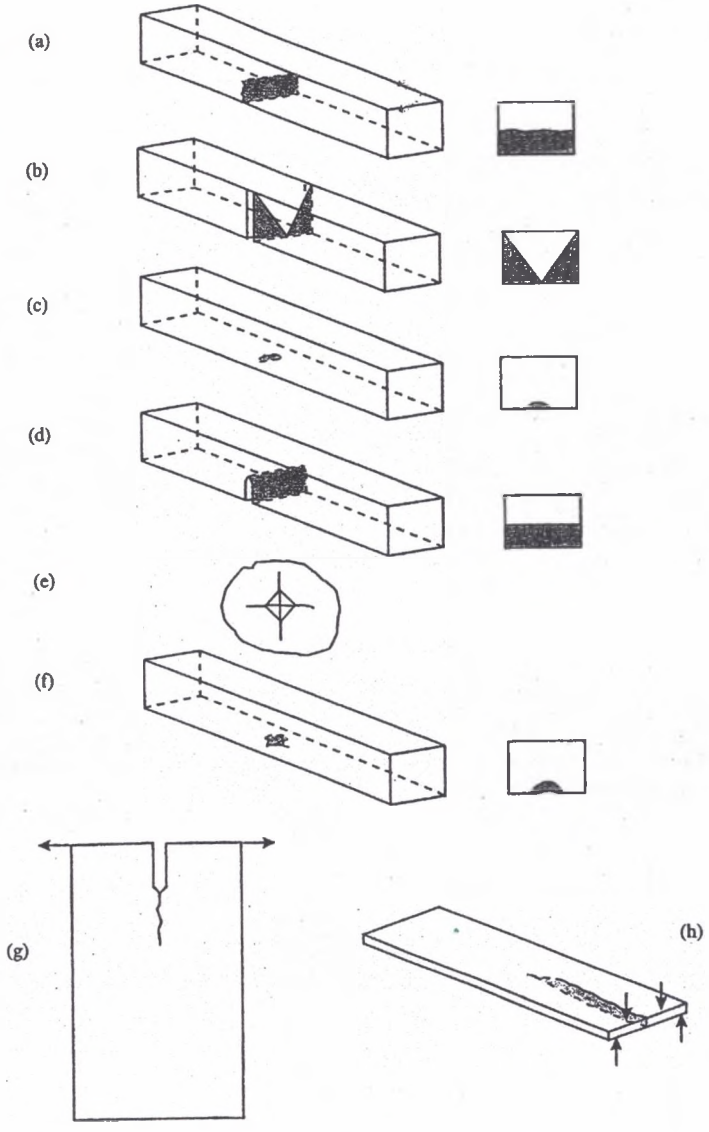

Fig. 1. Schematic representation of the various fracture toughness test methods [1]
Rys. 1. Ilustracja metod badania odporności na kruche pękanie [1]

3. Alternative techniques for fracture toughness evaluation

Problems connected with the effective and reliable use of the above presented experimental methods stimulated effort towards the development of empirical and semi-

empirical formulae describing the relationship between the critical stress intensity factor (K_{IC}) and other mechanical and physical properties that are much easier to measure and which finally led to the alternative techniques for fracture toughness evaluation. Some proposed empirical and semi-empirical qualitative relationships between the fracture toughness and other materials properties or microstructure parameters (which are not discussed later in this paragraph), are summarised in Table 1.

Table 1
The relationships between the fracture toughness and other material properties

No	Model – relationship	Sources
1	$WR \propto K_{IC}^{3/8} H^{1/2} (D_{WC})^{-1}$	[14]
2	$K_{IC} = 2{,}67 \times 10^7 \left(\frac{E}{H}\right)^{0,6} \left(1 + 0{,}012 \frac{E}{H}\right)^{-0,6} \varepsilon(I_\beta)^{0,6} H^{-1,5}$	[15]
3	$K_{IC} = 10^{-4}(1 - 7D_{WC})H + 11{,}7D_{WC} + 6$	[16]
Where:	WR - is wear resistance, mm^{-3} K_{IC} - is fracture toughness, MPa $m^{1/2}$ H - is hardness, MPa D_{WC} - is average WC grain size, μm E - is Young's modulus, MPS $\varepsilon(I_\beta)$ - is critical strain	

3.1. Correlation between flexural strength, macroscopic fracture surface area and fracture toughness

Yanaba and Hayashi [17] found that the fracture toughness (K_{IC}) of hard materials, such as the hardmetals and the ceramics are quantitatively related to the macroscopic fracture surface areas (S_{mf}) and flexural strength (σ_m) obtained from the bending test. They assumed that the elastic strain energy stored in the total volume of the testpiece just before the fracture should convert to the formation energy of the total fracture surface of the testpiece. The former elastic strain energy is proportional to σ_m^2 / E (E is Young's modulus and the latter is proportional to $S_{tf}(\gamma + P)$. (S_{tf} is the total true fracture surface area, γ is the surface energy per unit fracture surface area and P is the plastic deformation work per unit fracture surface area). The kinetic energy of flying fragments after the fracture was neglected. Therefore, the relation of $\sigma_m^2 / E \propto S_{tf}(\gamma + P)$ is considered to hold for each specimen when the size of the tsetpiece is constant. By applying the K_{IC} equation (1) and the Griffith-Orowan equation to the fracture of hardmetals and ceramics that occurs from one microstructural defect, the following equations are obtained, respectively:

$$K_{IC} = \phi_1 \sigma_m a \tag{2}$$

$$\sigma_m = \phi_2 \{2 (\gamma + P) E/(\pi a)\}^{\frac{1}{2}} \tag{3}$$

where a is the half length of the major axis of the fracture source, ϕ_1 and ϕ_2 are shape factors depending on both the size and shape of the fracture source and the size of the testpiece. Furthermore, the following equation is considered to hold for the fracture of hard materials, based on the law of conservation of energy at the moment of bending fracture.

$$\phi_3 \sigma_m^2 / E = \phi_4 S_{mf} (\gamma + P) \tag{4}$$

where ϕ_3 and ϕ_4 are the empirical correction factors.

The terms of $(\gamma + P)E$ and a ½ can be eliminated from the three equations 2, 3 and 4 by substituting Eqs (2) and (3) into Eq (4), and the resulting equation can be re-arranged as follows:

$$\sigma_m = \phi K_{IC} S_{mf}^{\frac{1}{2}} \tag{5}$$

where ϕ is a shape factor:

$$\phi = \{\pi\phi_4 /(2\phi_1^2 \phi_2^2 \phi_3)\}^{\frac{1}{2}} \tag{5a}$$

Yanaba and Hayashi [17] proved the validity of Eq (5) conducting experiments with hardmetals and ceramics (Table 2).

Table 2

Average flexural strength ($\bar{\sigma}_m$), fracture toughness (K_{IC}, by SEPB method, according to JIS R1607) and Vickers hardness (Hv) for hardmetals and Si_3N_4 base ceramic

Properties	WC-10Co	WC-10Co (HIPed)	Ni_3N_4
$\bar{\sigma}_m$ (GPa)	2,6	3,6	1,3
K_{IC} (MPa $m^{1/2}$)	11,5	10,7	3,1
Hv	1440	1410	1580

Equation (5), which was theoretically derived by taking into consideration the microscopic and macroscopic energy balance in the propagation of a crack or the formation of fracture surfaces, was proved to be compatible with experimental data. Authors conclude that there is a possibility that the K_{IC} of new hard materials can be estimated from data, i.e. (σ_m, $S_{mf}^{\frac{1}{2}}$) of only one flexural strength testpiece by using the experimental relationship between σ_m versus $S_{mf}^{\frac{1}{2}}$ found for several hard materials having various K_{IC}.

3.2. The hertzian indentation test for the evaluation of the fracture properties of brittle materials

In Hertzian contact, a pure elastic stress field is initially set up under a hard spherical indenter pressed into a flat surface of a brittle material. If the load is increased to a critical value, a ring crack initiates at the specimen surface just outside the edge of the contact circle [18-20]. As the load is increasing further, a cone crack develops under the surface (Fig 2). As it was demonstrated by Warren and Roberts [20], Lawn [18] and Zeng et al [19], Hertzian indentation is an attractive approach to measuring fracture toughness, although a widely applicable method has not yet been fully developed. By knowing the indentation load and the length of a fully developed cone crack, the Hertzian indentation approach can be used to determine the fracture toughness.

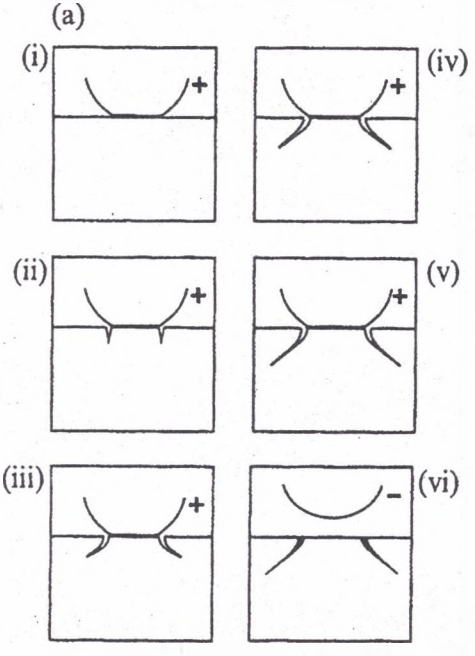

Fig. 2. Hertzian cone crack system. (a) Evolution of cone during complete loading (+) and unloading (-) cycle
Rys. 2. Układ stożkowych pęknięć Hertzowskich i jego zmiany podczas obciążania (+) i odciążania (-)

In order to calculate the stress intensity factor, it is necessary to find the Hertzian stress field solution [19, 21]. Huber derived a stress solution by simplifying the Hertz contact problem into a two-dimensional problem. However, it is now possible and appropriate to calculate the complete three-dimensional case without any simplifying assumptions.

Lundberg and Sjövall have provided the required complete three-dimensional stress solution for the elastic contact problem, derived from basic equations of elasticity combined with the proper boundary conditions for a semi-infinite body [19]. For the special case when the contact area is a circle, coordinates (r, θ, z), the stresses are:

$$\frac{\sigma_r}{\sigma_o} = -\frac{L^3 R^2 Z}{(L^4+Z^2)(1+L^2)^2} - (1-2\nu)\left[\frac{Z}{L(1+L^2)}\frac{1}{3R^2}\left(1-\frac{Z^3}{L^3}\right)\right] + \frac{Z}{L}\left[L(1+\nu)\arctan\left(\frac{1}{L}\right) - (1-\nu)\frac{L^2}{(1+L^2)} - 2\nu\right] \tag{6a}$$

$$\frac{\sigma_\theta}{\sigma_o} = -\frac{1-2\nu}{3R^2}\left[1-\left(\frac{Z^3}{L^3}\right)\right] + \frac{Z}{L}\left[L(1+\nu)\arctan\left(\frac{1}{L}\right) - (1-\nu)\frac{L^2}{(1+L^2)} - 2\nu\right] \tag{6b}$$

$$\frac{\sigma_z}{\sigma_o} = -\frac{Z^3}{L(L^4+Z^2)} \tag{6c}$$

$$\frac{\tau_{rz}}{\sigma_o} = -\frac{LRZ^2}{(L^4+Z^2)(1+L^2)} \tag{6d}$$

$$\frac{\tau_{r0}}{\sigma_o} = \frac{\tau_{z0}}{\sigma_o} = 0 \tag{6e}$$

where $\sigma_o = 3P/2\pi a^2$, L is the largest positive root of a quadratic equation and can be expressed as:

$$L = \sqrt{(\tfrac{1}{2})[R^2 + Z^2 - 1 + \sqrt{(R^2+Z^2-1)^2 + 4Z^2}]} \tag{7}$$

and $R^2 = X^2 + Y^2$, $X = \frac{x}{a}$, $Y = \frac{y}{a}$, $Z = \frac{z}{a}$ are normalised coordinates (Fig 3), and a is the radius of the contact area which is given by:

$$a^3 = \frac{4k\,PR^*}{3E_2} \tag{8}$$

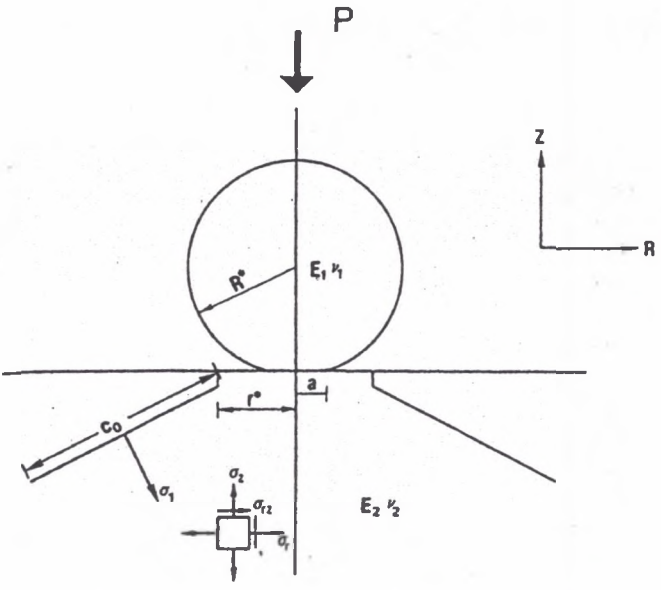

Fig. 3. Parameters of the Hertzian cone crack system, this diagram also indicates the symbols used in the calculations
Rys. 3. Układ stożkowych pęknięć Hertzowskich i oznaczenia stosowane do obliczeń

P is the indentation load, R* is the radius of the indenter, E_2 is the Young's modulus of the sample and

$$k = \frac{g}{16}\left[(1-\nu_1^2) + (1-\nu_2^2)\frac{E_2}{E_1}\right] \tag{9}$$

E_1 is the Young's modulus of the indenter, and ν_1 and ν_2 are the Poisson's ratios of the indenter and sample, respectively.

By suitable tensor transformations the directions and magnitudes of the principal stresses can be obtained. Two of the principal stresses σ_1 and σ_3, lie in the (r, z) plane θ = constant and their angles with the specimen surface are given by

$$\tan 2\alpha = \frac{2\tau_{rz}}{\sigma_z - \sigma_r} \tag{10}$$

The third principal stress σ_2, the hoop-stress, is everywhere perpendicular to the symmetry plane. The principal stresses can be expressed as

$$\sigma_1 = \frac{\sigma_r - \sigma\delta_z}{2} + \sqrt{\left(\frac{\sigma_r - \sigma_z}{2}\right)^2 + \tau_{zr}^2} \tag{11a}$$

$$\sigma_2 = \sigma_\theta \text{ (equation 6b)} \tag{11b}$$

$$\sigma_3 = \frac{\sigma_r+\sigma_z}{2} - \sqrt{\left(\frac{\sigma_r-\sigma_z}{2}\right)^2 + \tau_{zr}^2} \tag{11c}$$

Knowing the stress components σ_r, σ_θ and σ_z, and using equation (11), the principal stresses at any point inside the elastic body can be calculated.

Under the surface, directly below the indenter, there is a drop-shaped zone in which all principal stresses are compressive. Outside this zone σ_1 becomes tensile and the other remain compressive [19, 20]. How the tensile stress varies at the surface and below the surface can be summarised as follows: (1) the tensile stress reaches its maximum at the contact edge and falls off relatively slowly with increasing radial distance from the contact edge along the specimen surface.

Generally, when the length of a crack and the normal stress acting on this crack are known, the stress intensity factor at the crack tip can be found by a fracture mechanics approach. If the asymptotic field at a crack tip is defined by

$$\sigma_{ij} = \frac{K}{\sqrt{2\pi r}} \, fij(\theta) \tag{12}$$

the stress intensity factor for an internal crack of length $2c_o$ subject to a normal stress $\sigma_1(c)$, is

$$K = 2\left(\frac{c_o}{\pi}\right)^{\frac{1}{2}} \int_0^{c_o} \frac{\sigma_1(c)}{(c_o^2-c^2)^{\frac{1}{2}}} \, dc \tag{13}$$

Zeng et al [19] assumed that the principal tensile stress σ_1 is responsible for the formation of the ring crack and experimentally applied above approach for fracture toughness measurement of a ceramic matrix Al_2O_3/SiC composite (Table 3).

Comparing the results (Table 3) of the fracture toughness of the composite (6,7 MP $m^{1/2}$) with the values from SEPB method (9 MPa $m^{1/2}$) and the value from the Vickers indentation method (5,3 MPa $m^{1/2}$), the Hertzian indentation method gives a value which is within the range of reported values. Hertzian indentation has some of the same advantages as the Vickers indentation method (IF), i.e. it requires only small specimens. However, since the size of the cone crack cannot be directly measured at the surface, the specimen must be sectioned.

Table 3

Hertzian indentation results for the ceramic composite [19]

Load P (N)	Radius of contact area a^1 (mm)	Radius of the inner ring crack r^{*2}	Length of cone crack c_o^3 (mm)	Fracture toughness K^4 (MPa $m^{1/2}$)
686	0,125	0,151	0,098	8,0
735	0,128	0,160	0,105	6,0
784	0,131	0,172	0,115	6,0
833	0,134	0,165	0,138	6,0
882	0,136	0,173	0,142	6,8
931	0,139	0,168	0,150	7,2
980	0,141	0,170	0,158	6,7
1029	0,144	0,186	0,175	6,8
1127	0,148	0,195	0,198	6,4
Mean value at load range 600 - 1200 N : 6,7 MPa $m^{1/2}$				

1. Calculated from equation (8).
2. Measured on the surface.
3. Measured on the polished surface after sectioning.
4. Calculated from equation (13).

3.3. Toughness evaluation based on edge damage pattern

When a load is applied along the sharp edge of hard and brittle tools [10] or various other construction elements [22] cracks may initiate, propagate and eventually spall from the surface. On the other hand, in grinding or machining of brittle materials such as ceramics, optical glasses and hardmetals etc, flaking or chipping are often seen at the work edge where the cutting edge comes into contact with or separates from the work-piece [23]. This sudden controlled by fracture edge damage on the tools and on the work-pieces has been identified as a technologically significant problem in e.g. edge machining, edge mounting etc, and was named as edge cracking [22], edge spalling [22], edge flaking [24], edge chipping [25] and edge-break [23]. A number of attempts to devise novel methods of testing were made for a pragmatic way of ranking materials for toughness [10, 11, 22÷23] (Fig. 4) based on edge damage controlled by fracture.

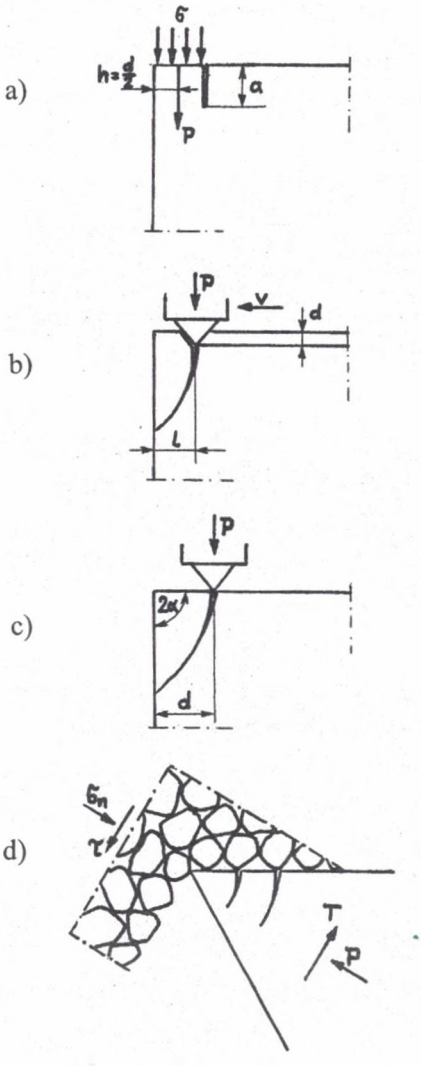

Fig. 4. Fracture toughness evaluation based on edge damage pattern: (a) edge spalling of brittle plate [22], (b) edge-break by scratch test [23], (c) edge chipping by single indenter [24,25] and (d) edge chipping in granular abrasive medium [10,11]

Rys. 4. Metody wyznaczania odporności na kruche pękanie oparte o ocenę zniszczeń krawędzi: (a) łuszczenie krawędzi kruchej płyty [22], (b) pękanie krawędzi podczas próby ryskowej [23], (c) odpryskiwanie krawędzi przez penetrator [24, 25], (d) wykruszanie krawędzi w środowisku ścierniwa [10, 11]

3.3.1. The edge cracking and spalling of brittle plate

Thouless et al [22] conducted tests aimed at background needed to analyse and predict the edge spalling behaviour and to allow definition of the criteria that dictate various aspects of edge cracking encountered in situations having practical importance. The experimental and theoretical part of the investigation has revealed that the loading used to conduct the experiments on the test specimens is complex. The test system depicted in Fig 4a consists of a plate containing a plane crack of length **a** at a depth **d**. The beam on the flank of the crack is subject to a uniform compressive stress, **σ**, parallel to the crack (or, equivalently, load per unit thickness **L/b = P**, exerted at a line of action, **d/2**). The stress state for this configuration is mixed mode, characterised by stress intensity factor, K_I and K_{II}.

Thouless et al [22] analysed both short (a << d) and long (a >> d) cracks asymptotic solutions but this review covers only asymptotic results for short cracks as more relevant for brittle materials. The stress intensity factors for short cracks may be obtained from the surface stresses as

$$\begin{aligned} K_I &\approx 1.12\,\sigma_{yy}\sqrt{\pi a} \\ K_{II} &\approx 1.12\,\sigma_{yx}\sqrt{\pi a} \end{aligned} \tag{14}$$

Specifically, for short cracks at depth **d**, subject to uniform edge compression

$$\begin{aligned} \frac{K_I\sqrt{d}}{P} &= 0{,}36\sqrt{\frac{a}{d}} \\ \frac{K_{II}\sqrt{d}}{P} &= 0{,}63\sqrt{\frac{a}{d}} \end{aligned} \tag{15}$$

The surface stress may also be used to estimate trends in the crack activation load, by requiring that fracture initiates from a distribution of pre-existing edge flaws. Then, the weakest link concept by Wiebull suggest that the fracture probability ϕ may be expressed as

$$-\ln(1-\phi) = \int_{2h}^{\infty}\left[\frac{\sigma_{yy}}{\varsigma_o}\right]^m \frac{dx}{h_o} \tag{16}$$

where m, ς_o and h_o are parameters that characterise the flaw population. Noting that, to a reasonable approximation

$$\sigma_{yy} \approx \frac{4}{(\pi^2-4)}\left[\frac{P}{x}\right] \tag{17}$$

the fracture load, at the median probability level ($\phi = ½$) may be readily derived as

$$P_c = \frac{m-1}{m}(\ln 2)^{\frac{1}{m}}\frac{(\pi^2-4)}{4}\,\xi_o\,(2h)^{\frac{m-1}{m}} \tag{18}$$

where $\xi_o = \varsigma_o h_o^{\frac{1}{m}}$. The fracture load is thus predicted to scale almost linearly with **h**.

Comparison between the experimental results conducted only on two transparent materials (PMMA and glass) and theory indicated that numerical discrepancies exist [22]. One possible contributor to the discrepancy arises from the loading configuration, the other from the specimen geometry. The method failed to deliver an easy and reliable solution for the edge toughness testing and hard materials ranking for fracture toughness.

3.3.2. The edge-break in machining of brittle materials

Inoue et al [23] studied the edge-break in the machining of brittle materials. Their experimental set-up included a scratch tester. Various kinds of brittle materials, ceramics which have different mechanical properties, were scratched by a conical diamond penetrator with scratch speed $v = 1$ mm/s and range of applied to penetrator load $P = 0{,}5\ N \div 14{,}7\ N$ (Fig. 4b) for the purpose of finding out some factors controlling the edge-break process. It was expected that the fracture toughness of work materials have a close relation to the occurrence of the edge-break. In order to treat the edge-break quantitatively the length of the edge-break "**l**" was defined as the distance from the nucleation point of a crack to the end face of the work-piece. Here, the edge-break nucleation point was assumed to be in the vicinity of the tip of the penetrator. A crack begins to extend towards the end face of the work-piece from the nucleation point to produce the edge-break (Fig. 4b).

The experimental results indicated the relation between the edge-break length, **l**, and the fracture toughness, $\mathbf{K_{IC}}$, with respect to the load applied, P. The lower the fracture toughness and the higher the applied load, the bigger the values of the edge-break length tend to be produced by the scratch test.

Finally, authors failed to establish a numerical correlation between the variables tested. The main reason that the mathematical equation or the experimental model of the edge-break phenomenon had not been presented was relatively poor coefficient of correlation between the experimental edge toughness indicator, **l**, and the actual value of fracture toughness measured by the Vickers indentation method.

3.3.3. Edge chipping of brittle materials by a single indenter

The strictly controlled process of edge damage in an experimental set-up in which a single hard indenter penetrates quasi-statically the sample of hard material can be used for ranking materials for toughness (Fig. 4c). In such an experiment the samples should have specified geometry and surface finish. The studies on edge toughness conducted by

McCormick [24], and Morrell and Gant [25] establish a testing procedure for this testing method.

Edge flaking (chipping) is mainly caused by quasi-static loading. The loading is sharp with considerable local plastic deformation prior to fracture, as evidenced by the existence of an indentation, so the fracture process is driven by an elastic/plastic stress field.

McCormick [24] in his investigation, tested various factors which were important from the point of view of the optimisation of the test procedure such as: the included angle of the edge, the surface roughness, the edge profile and the shape of the indenter. The critical load, P_c required for edge flaking was found to have a linear relationship with the distance, **d**, from the edge (Fig. 4c). The slope of the straight line produced from a least squares fit to the load and distance from edge data was found to be material dependent. This gradient was defined as the edge toughness of material, **M**.

$$M = \frac{P_c}{d} \cdot \frac{kN}{m} \tag{19}$$

The included angle of the edge was studied by McCormick [24] using a set of specimens with different included angles. Consequently, an experimental curve of edge toughness versus included angle was produced. This pattern of the edge toughness changes was explained by using a two-dimensional analysis proposed by Shepherd [26] which showed that the peak elastic tensile stress in the specimen implied a dependence on included angle for the edge toughness similar to that observed experimentally.

The maximum tensile stress for a point force varied from 0,255 P/C for a sector with included angle $2\alpha = 120^\circ$ to 1,136 P/C for 90° and to 2,87 P/C for a sector with included angle $2\alpha = 60^\circ$, where 2C is the thickness of the plate. As fracture propagation depends on the value of tensile stress the above relation suggests that fracture will occur at lower loads in test samples with included angle $2\alpha = 60^\circ$ than in samples with $2\alpha = 90^\circ$ or 120°.

Specimen roughness was investigated by using specimens prepared to various typical surface finishes. It was found [24] that there was no appreciable effect of surface roughness on the edge toughness or the shape of the flake over the range of finishes examined.

McCormick investigated also into the effect of the indenter on edge flaking. It was found that there was no statistically significant difference in the measured edge toughness using either a Rockwell "C" indenter or a Vickers indenter.

The concept of edge toughness was confirmed [24, 25] to be an important one. It is the technological parameter which describes the material's resistance to edge damage. As a

material parameter it should be related to other material parameters and it was found [24] that there is an empirical relationship between the edge toughness and the critical strain energy release rate, G_{IC} and the ratio of hardness, H, to Young's modulus, E. It was established that

$$\frac{M}{G_{IC}} = 14.13 + 894.6\,\frac{H}{E} \qquad r = 0{,}99 \tag{20}$$

where r is the correlation coefficient

M is the edge toughness, kN m^{-1}

G_{IC} is the critical strain energy release rate, Jm^{-2}

H is hardness, GNm^{-2}

E is Young's modulus, GN m^{-2}.

By rearranging equation (20) and using the identity

$$G_{IC} = \frac{K_{IC}^2}{E} \tag{21}$$

we find that

$$K_{IC} = \left(\frac{ME^2}{894.6H - 14.13E}\right)^{\frac{1}{2}} \tag{22}$$

where K_{IC} is the critical stress intensity factor, $MNm^{-3/2}$.

From this work the conclusion was drawn [24, 25] that there is a monotonic relationship between edge toughness and fracture toughness which shows scope for the use of edge toughness tests to provide information not just on the edge retention properties of a material but also on its fracture toughness.

4. Conclusion

Since the fracture toughness is often the major limiting parameter controlling the use of cermetals as drilling and cutting tools, there is a need for research aimed at increasing toughness without sacrificing wear resistance. In the paper (part I) a broad survey on fracture toughness measurement methods and alternative techniques for fracture toughness evaluation was presented, which in the next part (part II) leads to the new integrated method based on the concept of edge chipping.

REFERENCES

1. Roebuck B., Gee M., Bennett E. G., Morrell R.: Mechanical Tests for Hardmetals. NPL Good Practice Guide No 20, Teddington. 2000.
2. Morrell R.: Flexural Strength Testing of Ceramics and Hardmetals. NPL Good Practice Guide No 7, Teddington 1997.
3. Ogilvy M., Perrott C. M., Suiter J.: On the Indentation Fracture of Cemented Carbide – Survey of Operative Fracture Modes. Wear, 43, pp. 239-252, 1977.
4. Bennett E., Lay L., Morrell R., Roebuck B.: Microstructural Measurements on Ceramics and Hardmetals. NPL Good Practice Guide No 21, Teddington. 1999.
5. Laugier M. T.: Palmqvist indentation toughness in WC-Co composites. J. Mater. Sci. Lett. 6, pp. 897-900, 1987.
6. Jamison W. E.: Wear Control Handbook, Peterson M. B., Winer W. (eds), ASME, pp. 859-887, New York 1980.
7. Larsen-Basse J.: Wear of hardmetals in rock drilling. Powder Metallurgy, pp. 1-32, 1973.
8. Clark G. G. Principles of rock drilling and bit wear. Colorado SOM Quarterly, 77, pp. 1-91, 1982.
9. Guo H., Aziz N., Schmidt L. C. Rock cutting study using linear elastic fracture mechanics. Engineering Fracture Mechanics 5, pp. 771-780, 1992.
10. Ścieszka S F and Filipowicz K.: Materiały na narzędzia górnicze. Nowe trendy w technice badań. Wydawnictwo Politechniki Śląskiej, s. 1-106, Gliwice 2001.
11. Ścieszka S. F.: Wear transition as a means of fracture toughness evaluation of hardmetals. Tribology Letters 11, 3-4, pp. 185-194, 2001.
12. Fang Z., Griffo A., Lockwood G., Bitler J.: Properties of a high toughness cemented tungsten carbide composite. Advances in Powder Metallurgy and Particulate Materials, MPIF, New Jersey 10, pp. 123-131, 1999.
13. Roebuck B., Bennett E., Lay L., Morrell R.: Palmqvist toughness for hard and brittle materials. NPL Good Practice Guide No 9, Teddington 1998.
14. Wayne S., Baldoni J., Buljan S.: Abrasion and erosion of WC-Co with controlled microstructures. Tribology Transactions 33, pp. 611-617, 1990.
15. Laugier M.: A microstructural model relating fracture toughness and hardness in WC composites. Powder Metallurgy International 18, pp. 330-332, 1986.
16. Luyckx S., Richter V., Quigley D., Makhere L.: On the relationship between fracture toughness, hardness and grain size in WC-Co alloys, Proc. of the Int. Conf. on PM Materials, pp. 109-116, Kosice 1996.
17. Yanaba Y., Hayashi K.: Relation between fracture surface area of a flexural strength specimen and fracture toughness for WC-10 mass%Co Cemented carbide and Si_3N_4 ceramics. Materials Science and Engineering A209, pp. 167-174, 1996.
18. Lawn B.: Fracture of brittle solids. Cambridge University Press, pp. 249-306, 1995.
19. Zeng K., Breder K., Rowcliffe D. J.: The Hertzian stress field and formation of cone cracks. Acta Meetall. Mater. 40, pp. 2505-2605, 1992.
20. Roberts S. G.: Hertzian Testing of ceramics. British Ceramic Transactions 99, 1, pp. 31-38, 2000.
21. Li Y., Hills D. A.: The Hertzian cone crack. Transactions of the ASME 58, pp. 120-127, 1991.
22. Thouless M. D., Evans A. G., Ashby M. F., Hutchinson J. W.: The edge cracking and spalling of brittle plates. Acta Metall. 35, 6, pp. 1333-1341, 1987.

23. Inoue T., Kuniki T., Shibata J.: A study on the edge-break in machining of brittle materials. Bull. Japan Soc of Prec. Engg. 23, 1, pp. 10-16, 1989.
24. McCormick N. J.: Edge Flaking of brittle materials. PhD Thesis, NPL Teddington, pp. 121-264, 1993.
25. Morrell R., Gant A. J.: Edge chipping of hard materials. J. J. of Refractory Metals and Hard Materials, 19, pp. 293-301, 2001.
26. Shepherd W. M.: Stress systems in an infinite sector. Proc. Roy. Soc. A. 129, pp. 284-303, 1935.
27. Scieszka S.F.: Testing mechanical properties of materials for mining tools. Abrasive wear measurement methods – a review. Zeszyty Naukowe Politechniki Śląskiej (w druku).

Recenzent: Prof. dr hab. inż. Walery Szuścik

Omówienie

Praca zawiera obszerny przegląd metod stosowanych do badania odporności na kruche pękanie materiałów na ostrza narzędzi górniczych i wiertniczych. Najważniejszą grupą materiałów dla tego przeznaczenia są węgliki spiekane typu WC-Co. W ostatniej dekadzie producenci węglików spiekanych wprowadzili wiele ich modyfikacji, których końcowym efektem są produkty zaliczane do: nanospieków, kompozytów o gradiencie funkcjonalnym oraz kompozytów z wielowarstwowymi powłokami funkcjonalnymi. Ten rozwój stworzył potrzebę opracowania nowej i szybkiej metody badania najważniejszych własności powyższych materiałów, czyli ich odporności na kruche pękanie i odporności na zużywanie ścierne [27] oraz docelowo zaproponowanie metody integrującej oba mechanizmy niszczenia [27].